arXiv:1603.08449v2 [cond-mat.stat-mech] 18 Apr 2016

Linear and non-linear thermodynamics of a kinetic heat engine with fast transformations.

Luca Cerino, Andrea Puglisi, and Angelo Vulpiani
Istituto dei Sistemi Complessi - CNR and Dipartimento di Fisica, Università di Roma Sapienza, P.le Aldo Moro 2, 00185, Rome, Italy
(Dated: April 19, 2016)

We investigate a kinetic heat engine model constituted by particles enclosed in a box where one side acts as a thermostat and the opposite side is a piston exerting a given pressure. Pressure and temperature are varied in a cyclical protocol of period τ: their relative excursions, δ and ϵ respectively, constitute the thermodynamic forces dragging the system out-of-equilibrium. The analysis of the entropy production of the system allows to define the conjugated fluxes, which are proportional to the extracted work and the consumed heat. In the limit of small δ and ϵ the fluxes are linear in the forces through a τ-dependent Onsager matrix whose off-diagonal elements satisfy a reciprocal relation. The dynamics of the piston can be approximated, through a coarse-graining procedure, by a Klein-Kramers equation which - in the linear regime - yields analytic expressions for the Onsager coefficients and the entropy production. A study of the efficiency at maximum power shows that the Curzon-Ahlborn formula is always an upper limit which is approached at increasing values of the thermodynamic forces, i.e. outside of the linear regime. In all our analysis the adiabatic limit $\tau \to \infty$ and the the small force limit $\delta, \epsilon \to 0$ are not directly related.

PACS numbers: 05.70.Ln,05.40.-a,05.20.-y

I. INTRODUCTION

Thermodynamics, at its origins, received a crucial impulse from the study of heat engines [1]. It is interesting to realize that - after almost two centuries - engines still represent a relevant driving force towards new developments in this science. A challenging frontier in thermodynamics is the world of small and fast systems, where the assumptions of "quasi-reversible" transformations and the thermodynamic limit of statistical mechanics are not valid [2–4]. Obviously, "fast" thermodynamic transformations, i.e. those such that the typical cycle time τ is shorter than the slowest relaxation time of the system, constitute a key problem in the industry and, for this reason, have been under the scrutiny for many decades. In the 70's of the last century, several results were obtained in the so-called finite time thermodynamics [5], one of the foremost being the Curzon-Ahlborn (CA) estimate for the efficiency at maximum power [6]. Such an estimate has been revised in the recent years, with the introduction of new and more general classes of engines with respect to the original model considered by Curzon and Ahlborn [2, 7, 8]. A more recent wave of studies concerns the thermodynamics of systems with a "small" number N of degrees of freedom [9], motivated by the tremendous increase of resolution in the observation and in the manipulation of the micro-nano world, involving mainly biophysical systems and artificial machines [10]. The distinguishing feature of small systems is the relevance of fluctuations, which are negligible only when the number of constituents is very large, as for macroscopic bodies. The study of fluctuations in thermodynamics functions such as energy or entropy goes back to Einstein, Onsager and Kubo, but has recently taken an acceleration with the establishing of new results in response theory [11] and in the so-called stochastic thermodynamics [12, 13]. Such a turning point concerns the properties of fluctuations in system which are *far* from thermodynamic equilibrium, and therefore is intimately connected to the problem, mentioned before, of fast transformations. In a nutshell, modern stochastic thermodynamics addresses the finiteness of both transformation's time τ and system's size N.

In the literature about stochastic thermodynamics a prominent role is covered by models, often inspired by minimal experiments at the microscale, with very few degrees of freedom, where typically one has $N = 1$: the overdamped dynamics of the position of a colloid in a non-conservative (e.g. time-dependent) potential is a seminal prototype [14]. Only a few studies have discussed the non-trivial effects of inertia [15–17] where the relevant degrees of freedom are at least two (also with different parities under time-reversal). It is even more rare to find models with $N \gg 1$, still remaining in the domain of small N: for instance with an order of magnitude $N \sim 10^2$ fluctuations can still be relevant and possibly non-trivial, while the complexity of the dynamics is hugely raised. Such numbers are also closer to real biophysical applications with macromolecules, nanocapillaries, etc. [18]. On the front of the statistical mechanics of molecular models, an exception is certainly represented by the study in [19, 20], and by our more recent proposal in [4]. These papers investigate the dynamics of a gas model with N particles enclosed between a thermostat and a piston: the piston is controlled through a cyclic protocol of duration τ that defines operations similar to a heat engine. The basic equilibrium properties (i.e. thermodynamics and fluctuations, when $\tau \to \infty$) of that particular gas-piston system have been detailed in [21, 22]. In the study of the cyclic protocols the papers [19, 20]

do not take into account the piston's inertia and directly fix its (time-dependent) position during the cycle. In [4], on the contrary, we only fix the (time dependent) force acting on the piston, so that the piston's velocity is determined by the effect, mediated by inertia, of such a force and of the collisions with the gas' molecules. Because of a larger freedom in the piston's dynamics, this "machine" displays a much richer diagram of phases. In particular, the choice of τ determines different working regimes: engine, refrigerator and heat pump. In addition, also in view of an analysis of the linear regime of the engine similar to the one discussed in [20], in this model it is possible to disentangle the smallness of the external perturbation (represented by the excursion of forces and temperatures) with the slowness of the transformations (represented by the total time of the cycle).

In the present paper we study aspects of the model introduced in [4] which were not discussed or deepened in that paper. Among the new results, we introduce a formalization of the model in terms of fluxes and thermodynamics forces which allows to distinguish between a linear and a non-linear regime. In the linear regime, we get a matrix of Onsager coefficients which non-trivially depend on τ, a fact usually ignored in the recent literature. Along those lines, we can widen the study of the power optimization, considering different procedures of maximization (e.g. by varying different parameters, including the cycle duration τ) and comparing the results with the CA estimate for the efficiency.

The organization of the paper is sketched in the following. In Section II we illustrate the kinetic model and its coarse-grained approximations, which are useful in the rest of the paper, giving a quick overview of the results published in [4]. In Section III we introduce the thermodynamic analysis of the model, introducing the thermodynamic forces, the entropy production and the fluxes, focusing on the linear regime in the limit of small forces. In Section IV we discuss the efficiency at maximum power, under different protocols of maximization, and compare it with the Curzon-Ahlborn estimate. Finally we draw our conclusions and discuss perspectives for future studies in Section V.

II. THE ENGINE AND ITS PHASE DIAGRAM

In [4] we have studied a molecular model (MM) of engine. In the same paper we have also described an approximation of the MM called 2V model, indicating that two macro-variables are used to describe the coarse-grained dynamics of the engine. In view of the present study, it is useful to summarize the key results of that study.

MM The full model is an ideal gas of N point-like particles in a container with mass m, position $\mathbf{x}_i$ and momentum $\mathbf{p}_i$ ($\mathbf{v}_i = \mathbf{p}_i/m$), $i = 1 \dots N$. The real dimensionality of the box is not relevant, as the particles interact only with the piston and the thermostat: we consider only the $\hat{x}$ direction, assuming that the thermostat is at position 0 and the piston is at position $X(t) > 0$. The piston has mass M and momentum P and moves along $\hat{x}$ under the influence of the collisions with the gas particles and of an externally controlled force $\vec{F}(t) = -F(t)\hat{x}$. If $\mathbf{\Gamma} = (x_1, \dots, x_N, p_1, \dots, p_N, X, P)$ is the full phase space variable of the system, the Hamiltonian reads

$$\mathcal{H}(\mathbf{\Gamma}, t) = \sum_{i=1}^{N} \frac{p_i(t)^2}{2m} + \frac{P(t)^2}{2M} + F(t)X(t), \qquad (1)$$

with the additional constraints $0 < x_i(t) < X(t)$, $i = 1, \dots, N$, and $X(t) > 0$. The collisions with the piston are assumed to be elastic, i.e. conserve momentum and kinetic energy (see [4] for the details). When a particle collides with the wall at $x = 0$ it takes a new velocity v' with probability density

$$\rho(v') = \frac{m}{T_o} v' e^{-\frac{m v'^2}{2T_o}} \Theta(v), \qquad (2)$$

where $\Theta(v)$ is the Heaviside step function and we are measuring temperature T in energy units, i.e. $k_B = 1$ for the Boltzmann factor. When force and temperature are constant, the stochastic dynamics generated by this rule satisfies the detailed balance condition with respect to the canonical probability distribution $\rho(\mathbf{\Gamma}) \propto \exp(-\beta\mathcal{H})$.

Even if the particles do not directly interact, there is an indirect but relevant interaction through the piston, making N and Nm/M important parameters for the dynamics [23–26]. We study the system in a range of Nm/M close to ~ 1, meaning that there is a non-trivial interplay between the gas and the piston. The static study of the system (equilibrium at fixed F and T_0) can be found in [21, 22], yielding for the piston position average $\langle X \rangle^{eq} = (N+1)T_o/F$ and variance $\sigma_X^2 = (N+1)T_o^2/F^2$. The average instantaneous kinetic temperature of the gas $T(t) = \frac{1}{N}\sum_{i=1}^{N} m v_i(t)^2$, has ensemble average $\langle T \rangle^{eq} = T_o$ and ensemble variance $\sigma_T^2 = 2\,T_o^2/N$.

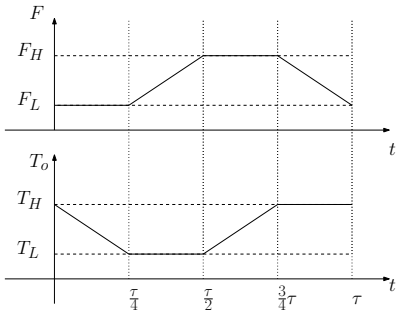

Figure 1. Force F and temperature T_0 as functions of time over a cycle period τ.

In order to obtain a heat engine (that is to extract mechanical work from the thermostat), it is necessary to vary F and T_o with time. Here we adopt the same

Segment	$\langle W\rangle$	$\langle Q\rangle$
I)	0	$\frac{3}{2}(N+1)(T_C-T_H)$
II)	$(N+1)T_C\ln\left(\frac{F_H}{F_L}\right)$	$-(N+1)T_C\ln\left(\frac{F_H}{F_L}\right)$
III)	0	$\frac{3}{2}(N+1)(T_H-T_C)$
IV)	$-(N+1)T_H\ln\left(\frac{F_H}{F_L}\right)$	$(N+1)T_H\ln\left(\frac{F_H}{F_L}\right)$

Table I. Table with the adiabatic values of Q and W in each segment of the Ericsson cycle. The average $\langle\cdot\rangle$ is intended over many realization of the cycle.

cyclical protocol - also known as "second type Ericsson cycle" - as in [4]: the duration of a cycle, τ, is divided in 4 sub-cycles, alternating two isobaric and two isothermal transformations. Temperature and force variations are always linear in time (see Fig. 1).

The main reason for such a protocol is to have a system which is always thermostatted, i.e. always near a canonical ensemble (at least for slow transformations): on the contrary, adiabatic transformations require a microcanonical analysis which may become less transparent. A similar model has been studied in [19] with a crucial difference: there the velocity of the piston is fixed at any time and cannot fluctuate (this choice corresponds to the infinite mass M limit). In [4] we have shown that a finite mass of the piston implies a rich phase diagram, due to the possibility of oscillations out of phase with respect to the external force.

The thermodynamic variables associated to energy variations are easily identified: the instantaneous internal energy $E(t)=\mathcal{H}(\mathbf{\Gamma}(t),t)$, the input power $\dot{W}(t)=\frac{\partial\mathcal{H}(t)}{\partial t}\Big|_{\mathbf{x}(t)}$ and the rate $\dot{Q}(t)$ of energy absorption from the thermal wall. Conservation of energy implies $\dot{E}(t)=\dot{Q}(t)+\dot{W}(t)$. For the Hamiltonian given in Eq. (1) one gets $\dot{W}=X\dot{F}$. Let us remark that this formula is different from the one obtained in standard thermodynamics, $\dot{W}=F\dot{X}$: this is due to the fact that we included the energy of the piston in the internal energy of the system [27]. For our choice of thermostat discussed before, the formula for the energy adsorption (heat flux) can be formally written as $\dot{Q}(t)=m\sum_i\delta(t-t_i)[(v_i'(t))^2-(v_i(t))^2]$ where t_i are the times of collisions between the gas particles and the thermostatting wall at $x=0$, whereas v_i and v_i' are the velocities before and after a collision respectively. In the following, unless differently specified, we use the symbols W and Q to mean a time-integral over a cycle, i.e. $W=\int_t^{t+\tau}\dot{W}(s)ds$ and $Q=\int_t^{t+\tau}\dot{Q}(s)ds$. Due to the stochastic nature of collisions and of the random choice of initial conditions, W and Q are random variables. Conversely, the symbols $\langle W\rangle$ and $\langle Q\rangle$ indicate the average work and heat per cycle computed over a long (single) run composed of a large number of cycles. Due to the periodic nature of the protocol the system will reach, after a transient, a periodic asymptotic state with a probability distribution in the full phase space depending on time only through $t'=t \mod \tau$. Therefore,

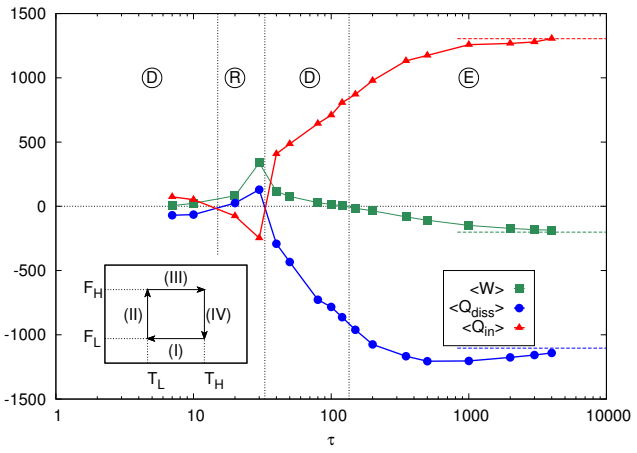

Figure 2. Average values per cycle of work W and heats Q_{diss}, Q_{in} as a function of the cycle period τ. Dashed horizontal lines represent the adiabatic value of such quantities. Inset: schematic of the cycle protocol in the space of parameters F, T_o. Other parameters are $F_L=180$, $F_H=220$, $T_C=11$, $T_H=13$, $m=1$, $M=100$, $N=500$.

thanks to the ergodic hypotheses, the average denoted by $\langle\cdot\rangle$, is equivalent to an average over the aforementioned periodic distribution.

The study of the thermodynamics of the engine in the quasi-static limit, i.e. assuming that the system is always at equilibrium: $X(t)=\langle X\rangle^{eq}_{F(t),T_o(t)}$ and $E(t)=\langle\mathcal{H}\rangle^{eq}_{F(t),T_o(t)}$, leads to the formula in Table I. During segments I) and III) no work is done on the system and the heats exchanged have same magnitude but opposite signs. Therefore, in the quasi-static limit $\tau\to\infty$, there is no net heat exchange with the intermediate reservoirs at temperature $T_C<T^*<T_H$. We do not expect this "heat symmetry" to hold when τ is finite. However, since the observed discrepancies are not large, in [4] we identified the input heat Q_{in} with the energy absorbed from the hot reservoir at T_H in segment IV), the dissipated heat Q_{diss} with the energy released into the cold thermostat T_C in sector II) and assumed $Q=Q_{in}+Q_{diss}$. In this paper a more refined definition (Eq. (28)) of input heat for the case of thermostats with continuous varying temperatures will be discussed.

If $\langle Q_{in}\rangle>0$ and $\langle W\rangle<0$, efficiency can be defined as

$$\eta=-\frac{\langle W\rangle}{\langle Q_{in}\rangle}. \tag{3}$$

The engine phase diagram In [4] we have numerically studied the MM (the numerical results of the MM reported in this paper are obtained from numerical simulations based on the common Verlet scheme with $\Delta t=0.001$), by restricting to a particular choice of the parameter and changing only the cycle duration τ. We have seen that in the $\tau\to\infty$ limit the thermodynamic predictions are recovered, but when τ is finite the system behaves differently: in particular there is a stall time

τ^* where $\langle W\rangle = 0$. For $\tau > \tau^*$ the system produces work as a standard heat engine ("E" phase). For smaller τ the system consumes work in two possible ways: as a refrigerator ("R" phase), i.e. by pushing heat from T_C to T_H ($\langle Q_{in}\rangle < 0$) or as a "dissipator" ("D" phase), i.e. with the heat going in the natural direction from T_H to T_C ($\langle Q_{in}\rangle > 0$). Since the heat extracted from the hot source, $\langle Q_{in}\rangle$ as a function of τ, crosses twice the 0 axis at times $\tau < \tau^*$, there are two changes of phases (from D to R and from R to D). The sequence of phases is well illustrated in Fig. 2. Interestingly, in the R phase the absorbed average work per cycle reaches a maximum. In the E phase the average output power $-\langle W\rangle/\tau$ reaches its maximum at some value τ_{mp} where the efficiency appeared to be close to the CA estimate $\eta_{CA} = 1 - \sqrt{T_C/T_H}$. A preliminary study of the fluctuations of W, Q_{in} and $\hat{\eta}$ was also present in [4]: the statistics of the work or heat per cycle appeared to be Gaussian in all phases, while the statistics of the fluctuating efficiency displayed a power law tail at large values, compatible with a -3 exponent.

2V model It is reasonable to expect that when the mass M of the piston is large its dynamics is smoother and possibly close to a continuous stochastic process. Based upon this idea, in [4], apart from an exactly derivable but still complicate model with three variables [28], we proposed a super-simplified model for only two "slow" variables: $X(t)$, $V(t)$:

$$\ddot{X} = -k(t)X + \mu(t)\dot{X} + \frac{F(t)}{M} + \sqrt{\frac{2\mu(t)T_o(t)}{2}}\xi(t). \quad (4)$$

where $k(t) = F(t)^2/[MNT_o(t)]$, $\mu(t) = 2F(t)\sqrt{2m/[M^2\pi T_o(t)]}$ and $\xi(t)$ is white noise with zero average and unitary variance. We assumed the parameters to vary in a way which is more convenient for calculations (setting $\omega = 2\pi/\tau$ for the engine frequency)

$$\begin{aligned} F(t) &= F_0(1 + \epsilon\cos(\omega t)), \\ T(t) &= T_0(1 + \delta\sin(\omega t)). \end{aligned} \quad (5)$$

In the linear limit $\epsilon \sim \delta \ll 1$, a perturbative expansions [4] leads to a formula for the average trajectory and work performed over a cycle of duration τ, i.e. of frequency ω:

$$\langle X(\omega,t)\rangle = \frac{NT_0}{F_0} + A(\omega)\{\delta\sin[\omega t + \phi(\omega)] - \epsilon\cos[\omega t + \phi(\omega)]\}, \quad (6)$$

$$\langle W(\omega)\rangle = F_0\pi\epsilon A(\omega)\left[\epsilon\sin\phi\left(\omega\right) - \delta\cos\phi\left(\omega\right)\right], \quad (7)$$

where

$$\begin{aligned} A(\omega) &= \frac{NT_0F_0}{\sqrt{8mT_0F_0^2\omega^2 + \left(F_0^2 - \frac{MNT_0}{\pi}\omega^2\right)^2}}, \\ \phi(\omega) &= \arctan\left(\frac{2NF_0T_0\omega}{F_0^2 - MNT_0\omega^2}\sqrt{\frac{2m}{\pi T_0}}\right). \end{aligned} \quad (8)$$

The 2V model reproduces qualitatively the numerical results of the MM, but shows quantitative discrepancies. A study of the time-autocorrelations of the piston position or velocity in the MM, even at equilibrium, reveals many relaxation times [22]: such a study suggests that a reasonable number of variables is 5 (for instance some average properties of the gas, such as average position, velocity and kinetic energy could be added to the 2V model), but a multivariate stochastic process with so many variables (and a consequently large number of parameters) is far from our aim. The question about the linearity of the model is also open [29].

III. LINEAR REGIME

A. General results

Many general results [2, 30, 31] regarding the performance of finite-time heat engines are obtained within the framework of irreversible thermodynamics [32]. For this reason and also for having a different insight into the physics of our model, in this Section we recall some basic notions on the Onsager formulation of out-of-equilibrium processes in order to fit our molecular model into this formalism.

Every irreversible process is characterized by a non-negative entropy production (we consider the quantities integrated in time on a cycle period τ) Σ which, in turn, can be expressed as the sum of n products of some thermodynamic (time-integrated) fluxes J_i with the associated thermodynamic forces f_i [32]:

$$\Sigma = \sum_{i=1}^{n} J_i f_i. \quad (9)$$

The entropy production and all the fluxes are expected to vanish at equilibrium (i.e. when there are no thermodynamic forces). Consequently, when the forces are small, the fluxes can be expressed as linear combinations of the forces,

$$J_i = \sum_{k=1}^{n} L_{ik} f_k, \quad (10)$$

where L_{ik} are the so-called *Onsager coefficients*. Thus, in the linear regime, the entropy production rate is a quadratic form of the thermodynamic forces,

$$\Sigma = \sum_{i,k=1}^{n} L_{ik} f_i f_k. \quad (11)$$

The matrix of Onsager coefficients (*Onsager matrix*), given the positivity of Σ, must be positive-semidefinite.

In many physical problems the identification of fluxes and forces is unambiguous: that is not the case in the problem we are considering [33, 34]. Our model belongs

to the class of hamiltonian systems $\mathbf{x}$ with Hamiltonian $\mathcal{H}(\mathbf{x}(t), F(t))$ and coupled to a thermostat at the time-dependent temperature $T(t)$. Both $F(t)$ and $T(t)$ are periodic functions of time, with period τ. Since the thermostatting dynamics satisfies, at every time t, the detailed balance condition with the equilibrium (Gibbs) distribution at temperature $T(t)$, the total average entropy production (see Appendix A) of the system reads

$$\Sigma(\tau) = -\int_0^\tau \frac{\langle \dot{Q}(t) \rangle}{T(t)} dt \geq 0, \tag{12}$$

where $\dot{Q}$ is the rate of heat absorption from the thermostat. To obtain a decomposition analogous to Eq. (9), it is useful to express the temperature, following [35], as

$$T(t) = \frac{T_0(1-\delta^2)}{(1+\delta) - 2\delta\gamma(t)}, \tag{13}$$

where $T_0 = (T_H + T_C)/2$ and

$$\delta = \frac{T_H - T_C}{T_H + T_C}. \tag{14}$$

The time-dependence of $T(t)$ is expressed through the function $0 \leq \gamma(t) \leq 1$, so that $\gamma(t) = 1 \iff T(t) = T_H = T_0(1+\delta)$ and $\gamma(t) = 0 \iff T(t) = T_C = T_0(1-\delta)$. We will also use the notation $F_0 = (F_H + F_L)/2$ and

$$\epsilon = \frac{F_H - F_L}{F_H + F_L}, \tag{15}$$

to indicate, respectively, the intermediate force and the relative excursion. By plugging Eq. (13) into Eq. (12) and using $\langle W \rangle + \langle Q \rangle = 0$ one gets

$$\Sigma(\tau) = \frac{\langle W \rangle}{T_0(1-\delta)} + \delta \left(\frac{2}{T_0(1-\delta^2)} \int_0^\tau \langle \dot{Q} \rangle \gamma(t) \right). \tag{16}$$

By interpreting ϵ and δ as the two (adimensional) independent thermodynamic forces, or affinities, acting on the system, and recalling that $\langle W \rangle \propto \epsilon$ for small ϵ, one gets an expression analog to Eq. (9):

$$\Sigma(\tau) = \epsilon J_1(\tau) + \delta J_2(\tau), \tag{17}$$

where

$$J_1(\tau) = \frac{\langle W \rangle}{\epsilon T_0(1-\delta)}, \tag{18}$$

$$J_2(\tau) = \frac{2}{T_0(1-\delta^2)} \int_0^\tau \langle \dot{Q} \rangle \gamma(t). \tag{19}$$

The physical meaning of J_2 can be understood by analyzing the limiting case where $T(t)$ is a square wave function between T_C and T_H (i.e. when $\gamma(t)$ assumes only the values $\gamma = 1$ or $\gamma = 0$): in this case J_2 is proportional to the heat Q_H exchanged with the hot thermostat. It is worth noticing that expressions different from Eq. (13) can lead to different (legit) definition of fluxes: nonetheless, this decomposition is particularly suited for an analysis of the efficiency at maximum power (see Sec. IV).

For small values of ϵ and δ, i.e. in the linear regime, the fluxes are linear function of the forces

$$J_i(\tau) = L_{i1}(\tau)\epsilon + L_{i2}(\tau)\delta, \qquad i = 1, 2, \tag{20}$$

where the Onsager coefficients L_{ij} non-trivially depend on the total time τ of the transformation.

B. Reciprocity relations and behavior far from the linear regime

We now discuss a generalization of the Onsager reciprocity relations for systems undergoing cyclical transformations, proposed in in Ref. [35] . For each protocol determined by $T(t)$ and $F(t)$, it is possible to construct its "time-reversed" counterpart $\tilde{T}(t) = T(\tau - t)$ and $\tilde{F}(t) = F(\tau - t)$: if we indicate with $\tilde{\cdot}$ quantities measured in the time-reversed cycle, the following relation is a direct consequence of the reversibility of the microscopic dynamics:

$$L_{12}(\tau) = \tilde{L}_{21}(\tau). \tag{21}$$

For the Ericsson protocol described in Sec. II the time reversal transformation can be obtained by taking the same form of the protocol for T and F with an (inessential) global shift of phase $t_0 = \tau/2$ and inverting the sign of the force difference $\epsilon \to -\epsilon$. For this reason $\tilde{L}_{21} = -L_{21}$, i.e.

$$L_{12}(\tau) = -L_{21}(\tau). \tag{22}$$

In Fig. 3 the results of a measurement of J_1 and J_2 for different values of ϵ and δ in molecular dynamics simulations of the MM are reported. By fixing, respectively, $\delta = 0.05$ or $\epsilon = 0.05$, J_2 and J_1 are plotted as functions of ϵ and δ. A linear dependence is obtained for small values of the thermodynamic forces: moreover, the data are compatible with the hypothesis of two linear relations with opposite coefficients describing the functional dependence of J_1 on δ and of J_2 on ϵ (straight lines in Fig. 3). The measurement also confirms the fact that the Onsager coefficients have a non trivial dependence on the total time of the transformation τ (inset of Fig. 3). In Fig. 4 we report a measurement of J_1 as a function of ϵ for different values of δ: since the curves are parallel straight lines, the Onsager coefficient L_{11} does not depend on the value of δ (analogous results, not reported here, can be obtained for all the Onsager coefficients).

In Fig. 5 we study the limits of the linear behavior of the MM: by taking $\delta = \epsilon$, we report the average work divided by ϵ^2 as a function of τ for different values of ϵ. In the linear regime the different curves, when rescaled, must superimpose: this is the case, of course, for small values of ϵ. At larger values of ϵ the appearing discrepancies are not uniform in τ. In particular we remark that

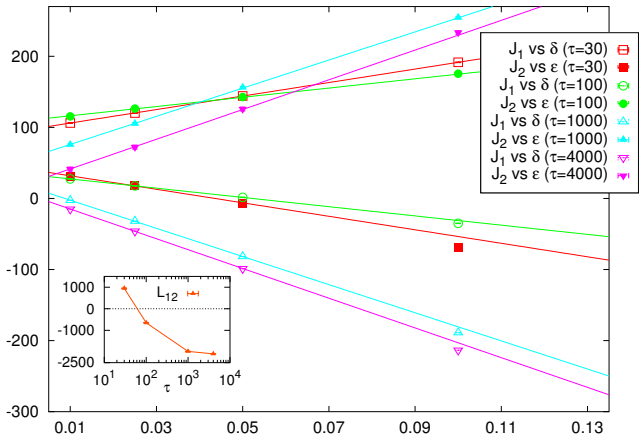

Figure 3. Thermodynamic currents J_1 (empty symbols) and J_2 (solid symbols) as functions, respectively, of thermodynamic forces δ and ϵ for different values of τ. Straight lines are obtained by fitting the two data sets at the same τ with two linear functions with slope L_{12} and $-L_{12}$ respectively: for this reason, lines with the same color have opposite slope. Inset: Off-diagonal Onsager coefficient L_{12} obtained with the above procedure as a function of τ. All the other parameters are the same of Fig. 2.

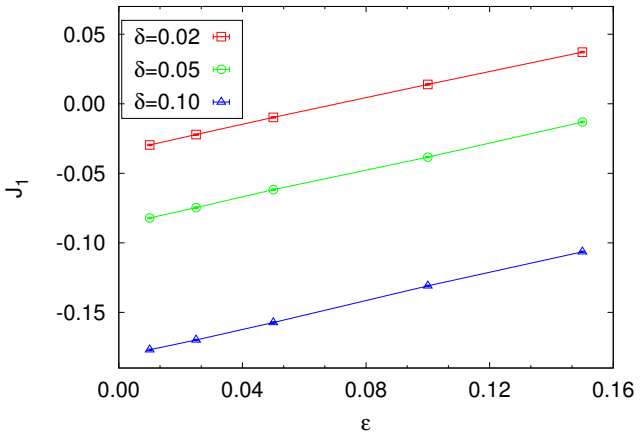

Figure 4. The thermodynamic current J_1 as a function of ϵ for different values of δ at $\tau = 500$. Other parameters are the same of Fig.2

around the maximum of $\langle W \rangle$ the separation is much more prominent (also signaled by the appearance of a second local maximum for $\epsilon \geq 0.25$). Note that the non-linearity appears also in the large τ limit, since higher order terms of the expansion of the quantity $\log\left(\frac{1+\epsilon}{1-\epsilon}\right)$ in the adiabatic formula of work (see Table I) become relevant. Unfortunately an analytic description of the non-linear regime is not yet available and the interesting features of such a regime will hopefully be the subject of future investigations.

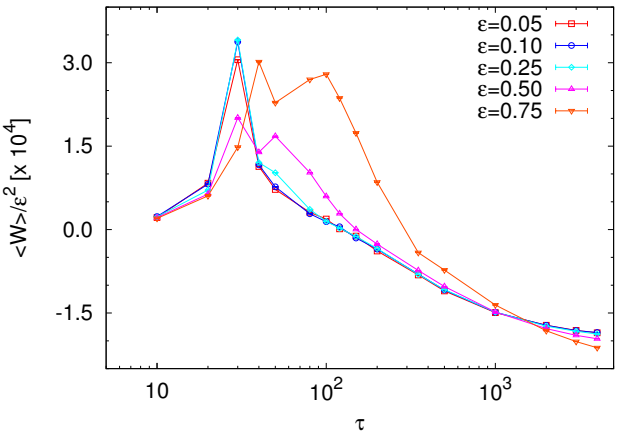

Figure 5. The average work per cycle, divided by ϵ^2 is reported as a function of τ for different values of ϵ. The other parameters are $\delta = \epsilon$, $F_0 = 200$, $T_0 = 12$, $N = 500$, $M = 100$, $m = 1$.

C. Analytic expression of the Onsager coefficients in the 2V model

In the simplified 2V model, Eq. (4), it is possible to obtain an explicit expression for the above mentioned Onsager coefficients L_{ij}. By plugging Eq. (7) into definition (19) one immediately gets the linear expansion for J_1, i.e.

$$J_1(\tau) = \frac{F_0}{T_0}\pi A\left(\frac{2\pi}{\tau}\right)\left(\epsilon \sin\phi\left(\frac{2\pi}{\tau}\right) - \delta\cos\phi\left(\frac{2\pi}{\tau}\right)\right). \tag{23}$$

In order to get the corresponding expansion for J_2, we start by plugging the protocol $T(t) = T_0(1 + \delta\sin(2\pi t/\tau))$, Eq. (5), into Eq. (13) and get

$$\gamma(t) = \frac{1}{2}\left(1 + \sin\left(\frac{2\pi}{\tau}t\right)\right) + \mathcal{O}(\delta). \tag{24}$$

To obtain an explicit expression for $\langle \dot{Q} \rangle$ it is necessary to substitute the asymptotic solution for $\langle X \rangle$, Eq. (6) into the expression for energy $\langle E(t) \rangle = NT_o(t)/2 + M\langle \dot{X} \rangle^2/2 + F\langle X \rangle$, and then use the definition of heat $\langle \dot{Q} \rangle = \langle \dot{E} \rangle - \dot{F}\langle X \rangle = \mathcal{O}(\epsilon, \delta)$. Retaining only first order terms in ϵ and δ of Eq. (19) gives the following expression for J_2:

$$J_2 = \frac{\pi F_0}{T_0} A\left(\frac{2\pi}{\tau}\right)\left(\epsilon\cos\phi\left(\frac{2\pi}{\tau}\right) + \delta\sin\phi\left(\frac{2\pi}{\tau}\right)\right). \tag{25}$$

In summary, the Onsager matrix takes the form

$$L = \frac{F_0}{T_0}\pi A\left(\frac{2\pi}{\tau}\right)\begin{pmatrix} \sin\phi\left(\frac{2\pi}{\tau}\right) & -\cos\phi\left(\frac{2\pi}{\tau}\right) \\ \cos\phi\left(\frac{2\pi}{\tau}\right) & \sin\phi\left(\frac{2\pi}{\tau}\right) \end{pmatrix} \tag{26}$$

The anti-reciprocal relation $L_{12} = -L_{21}$ in the Onsager matrix is due to the fact that the protocol used in the

2V model (Eq. (5)) behaves, under time-reversal, in the same way as the Ericsson protocol. We can also get a very simple expression for the total entropy production,

$$\Sigma(\tau) = \frac{\pi F_0}{T_0} A\left(\frac{2\pi}{\tau}\right) \sin\phi\left(\frac{2\pi}{\tau}\right)(\epsilon^2+\delta^2), \qquad (27)$$

which, as expected, is always positive because $A(\omega) \geq 0$ and $0 \leq \phi(\omega) \leq \pi$.

IV. EFFICIENCY AT MAXIMUM POWER: LINEAR REGIME AND BEYOND

The aim of this Section is to study the efficiency at maximum power of our engine comparing three different levels of approximation: numerical simulations of the full Molecular Model, numerical solutions of its coarse-grained 2V version, and analytical solutions of the 2V model for small values of ϵ and δ (i.e. when fluxes are linear in the forces).

First, we need to find a suitable definition of efficiency η for our case. Usually the efficiency of a heat engine working at contact with two thermostats (at temperatures $T_C < T_H$) is simply the ratio of the output work divided by the energy absorbed from the hotter thermostat Q_{in}. For transformations that involve thermostats at temperatures ranging continuously in the interval $T_C < T(t) < T_H$, the input heat must be redefined [35] as

$$Q_{in} = \int_0^\tau \dot{Q}(t)\gamma(t)dt, \qquad (28)$$

where τ is the total time of the transformation and $\gamma(t)$ is the function appearing at the denominator of the right-hand side of Eq. (13). This definition comes from the observation, already reported in the previous section, that Eq. (28) gives the correct result in the simple case of two thermostats at T_C and T_H: moreover for the Ericsson protocol this expression reduces, in the quasi-static limit, to the heat extracted from the hot reservoir T_H.

From this definition, we get the expression for the efficiency of the engine,

$$\eta = \frac{-\langle W\rangle}{\langle Q_{in}\rangle} = -\frac{2\epsilon J_1}{(1+\delta)J_2}, \qquad (29)$$

where we used Eqs. (18) and (19) to recast the expression in terms of the thermodynamic currents J_1 and J_2. When the total average entropy production Σ, Eq. (17), vanishes, it is straightforward to prove that the efficiency assumes the Carnot value $\eta_C = 1 - T_c/T_H = 2\delta/(1+\delta)$. In the 2V model, the entropy Eq. (27), can vanish only for $\phi = 0$, i.e. in the adiabatic limit $\tau \to \infty$ (or in the trivial, non-interesting case $\tau = 0$). It is quite reasonable to assume that, also in the general case, a vanishing entropy can be only obtained by varying very slowly the external parameters. As a consequence, the power corresponding to a maximally efficient engine must be zero. For this reason, in order to characterize the performance of the engine, we will study the efficiency at maximum power (EMP) $\tilde{\eta}$, i.e the efficiency corresponding to a choice of the external parameters that maximizes the output power. In the last decades, a series of important results were obtained regarding the EMP: perhaps the most notable is that, under some rather general assumptions [2, 6], a universal bound for the EMP is given by the so-called Curzon-Ahlborn efficiency η_{CA},

$$\tilde{\eta} \leq \eta_{CA} = 1 - \sqrt{\frac{T_C}{T_H}} \approx \frac{1}{2}\eta_C + \mathcal{O}(\eta_C^2). \qquad (30)$$

We now investigate the validity of such a bound, and compare our results with other recent works.

In our models the output power:

$$\mathcal{P} = -\frac{\langle W\rangle}{\tau} \qquad (31)$$

depends on the details of the model (N, M, m) as well as on the choice of the external protocol $(T_0, F_0, \epsilon, \delta, \tau)$. Since the engine working state consists in a perturbation of the equilibrium state determined by T_0 and F_0, it appears quite natural, in order to maximize $\mathcal{P}$, to fix N, m, M, T_0 and F_0. Moreover, since η_C and η_{CA} only depend on the value of δ, we also fix the temperature difference and therefore maximize the two-variables function $\mathcal{P}(\epsilon, \tau)$.

A. Linear regime

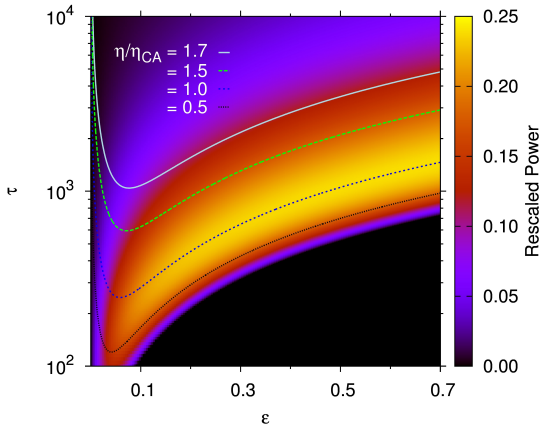

Figure 6. *2V model, linear appoximation*: contour plot of rescaled $\mathcal{P}(\epsilon, \tau)$ as a function of τ and ϵ. The power is rescaled by the factor $w_{ad}^{2V} = \epsilon\delta N T_0 \pi/100$ evaluated in $\epsilon = 0.1$, $\delta = 1/12$, $N = 500$, $T_0 = 12$, $w_{ad}^{2V} \approx 1.57$. Continuous line represents the set of points (ϵ, τ) where η/η_{CA} is constant.

In Fig. 6 the linear approximation for the output power in the 2V model (obtained by plugging Eq. (7) into Eq.

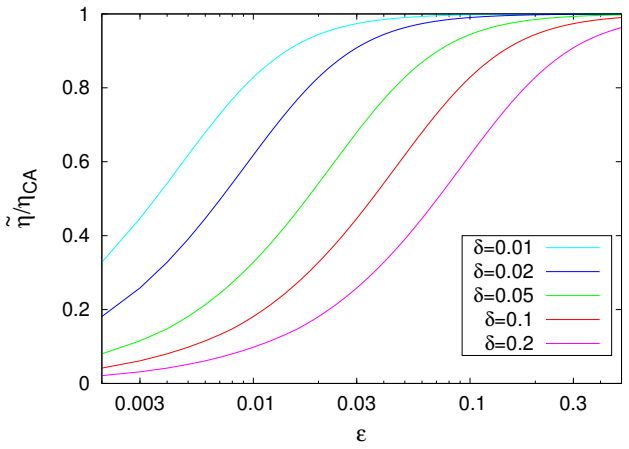

Figure 7. *2V model, linear approximation*: ratio of efficiency at maximum (with respect to τ) power $\tilde{\eta}$ and Curzon-Ahlborn efficiency η_{CA}, as a function of ϵ for different values of δ. Other parameters are $N = 500$, $M = 100$, $m = 1$, $T_0 = 12$, $F_0 = 200$.

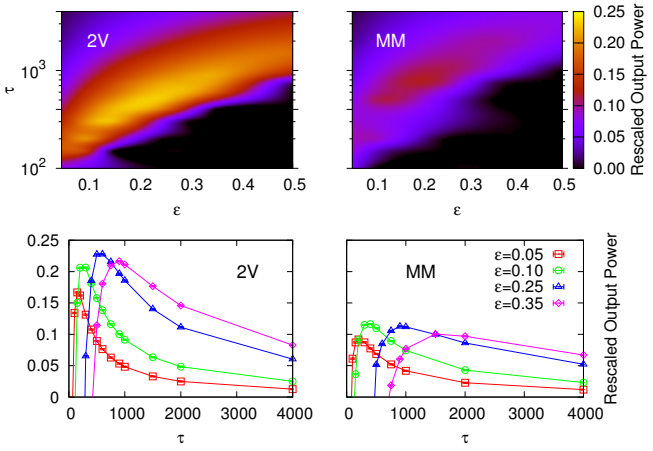

Figure 8. *Left: 2V model solved numerically, right: simulations of the MM.* Top panels: colour plot of the rescaled output power. Bottom panels: the rescaled output power as a function of τ for different values of ϵ. Parameters are the same in 2V and MM simulations: $\delta = 1/12$, $N = 500$, $M = 100$, $m = 1$, $F_0 = 200$, $T_0 = 12$. The power in MM simulation is divided by the quantity $w_{ad}^{MM} = 0.02\, N\, T_0\, \delta \ln\left((1+\epsilon)/(1-\epsilon)\right)$ in $\epsilon = 0.1$, $w_{ad}^{MM} \approx 2.007$. In the 2V model the rescaling factor is $w_{ad}^{2V} = \epsilon\delta N T_0 \pi/100$ which, in $\epsilon = 0.1$ gives $w_{ad}^{2V} \approx 1.57$

(31)) is plotted as a function of ϵ and τ. In view of a comparison between the results in the 2V model and in the molecular model, whose protocols are slightly different, we rescaled the work and the power so that, for $\epsilon = 0.1$ the asymptotic value for work in the limit $\tau \to \infty$ is fixed to $\lim_{\tau\to\infty} W_{rescaled}(\epsilon = 0.1, \tau) = 100$. The plot shows that (in this linear approximation) the power does not reach a global maximum at a unique value of (τ, ϵ). Indeed, there exists a curve $\tau_{mp}(\epsilon)$ consisting of τ-maxima points, i.e. where $\partial_\tau \mathcal{P} = 0$. The maximum power curve $\mathcal{P}[\epsilon, \tau_{mp}(\epsilon)]$ saturates to a constant value for increasing ϵ. In addition we also note that $\tau_{mp}(\epsilon)$ is an increasing function of ϵ, eventually saturating at the value $\lim_{\epsilon\to 1} \tau_{mp} \approx 1500$. In the plot we have also shown the curves at constant η: it is interesting to notice that the $\tau_{mp}(\epsilon)$ approaches the curve where $\eta = \eta_{CA}$ at increasing ϵ.

The EMP curves, $\tilde{\eta}(\epsilon, \tau_{mp}(\epsilon))$ for different values of δ are shown in Fig. 7: we observe that - consistently with the previous observation - the CA efficiency is only reached for large values of ϵ where, in principle, the linear approximation is no more reliable. However, by decreasing δ a faster convergence toward the CA efficiency is observed: this suggests the possibility to observe $\tilde{\eta} = \eta_{CA}$ even in the linear regime.

Let us remark again that in our system it is possible to separate the time τ of the transformation from the small force limit (small ϵ and δ): this means that we are able to consider a linear approximation (and construct the corresponding τ-dependent Onsager matrix) which is valid, in the small $\epsilon - \delta$ limit, at every value of τ. On the contrary, in many recent papers (see e.g. [20, 36]) one of the small thermodynamic forces must be the inverse of the time of the transformation τ.

B. Non-linear regime

The absence of an absolute maximum for the power, however, appears only to be a consequence of the linear approximation used to solve the 2V equations. Indeed, by performing numerical integration of the full 2V model (Eq. (4)) and simulations of the MM, we observe a rather different situation, which is reported in Fig. 8: the two top panels represent the color map of the functions $\mathcal{P}(\epsilon, \tau)$ for the two models, the two bottom panels show some sections $\mathcal{P}(\epsilon^*, \tau)$ vs τ, for some values of ϵ^*. By analyzing these last plots, we observe that the maximum power increases when going from $\epsilon = 0.1$ to $\epsilon = 0.25$ and then decreases again in $\epsilon = 0.35$. This suggests that is indeed possible, at least numerically, to find a specific value for ϵ and τ corresponding to the global maximum power. The only significant difference between the 2V model and the MM is that the output power is smaller, in general, than the one obtained in the 2V model.

In Fig. 9 we focus on the MM and report the same output power as a function of the efficiency (which, interestingly, is a bijective function of τ). We observe that, at every value of ϵ, the maximum power is attained at a value $\eta < \eta_{CA}$: moreover the global maximum power corresponds to an efficiency that is approximately the 70% of the Curzon-Ahlborn efficiency (i.e. 35% of the Carnot efficiency). The Curzon-Ahlborn efficiency seems to be approached for larger values of ϵ. A comparison between the EMP measured in the numerical simulations of the MM and the corresponding result in the 2V model (inset of Fig. 9), shows that the simplified model overestimates the actual value of $\tilde{\eta}$.

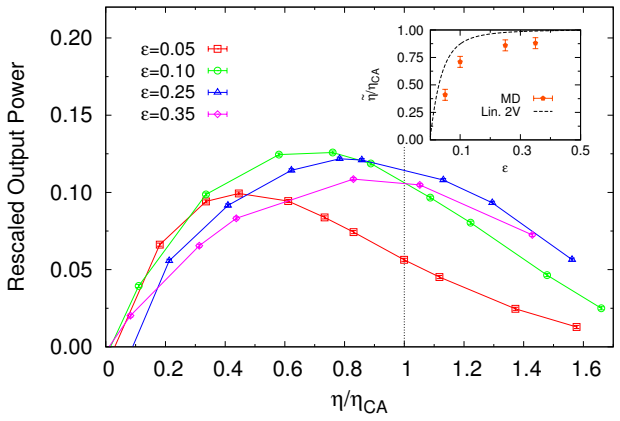

Figure 9. *Simulations of the MM*: the rescaled output power is reported as a function of the rescaled efficiency η/η_{CA} for different values of ϵ. The rescaling factor for power is $w_{ad}^{MM} \approx 2.007$ and $\eta_{CA} = 1 - \sqrt{(1+\delta)/(1-\delta)}$. Inset: comparison between numerically solved 2V model and simulations of the MM for the relative EMP $\tilde{\eta}/\eta_{CA}$ is reported as a function of ϵ. Other parameters are the same as in Fig. 8.

We wish to spend a few words about the observed lower value of the EMP with respect to the CA efficiency. We see that it is a consequence of the widening of the space of parameters [17]. In Ref. [2] (and its generalization to non-symmetric Onsager matrices in Ref. [35]), it is proved that, for fixed Onsager coefficients (i.e. for fixed τ) η_{CA} is reached whenever the value

$$q = \frac{L_{12}L_{21}}{L_{11}L_{22} - L_{12}L_{21}} \tag{32}$$

is close to $q = 1$ ("tight coupling" hypothesis). When the Onsager matrix is τ-dependent, the variable q is a function of τ, $q = q(\tau)$. Suppose the existence of a value of $\tau = \tau_0$ such that the tight-coupling hypotesis is verified $q(\tau_0) \simeq 1$: then, by denoting with ϵ_0 the value of ϵ that maximizes the power at $\tau = \tau_0$ (with respect to ϵ), we will obtain $\eta(\tau_0, \epsilon_0) = \eta_{CA}$. On the other hand, the global maximum power in the (τ, ϵ)-plane may occur in a point (τ_1, ϵ_1) for which the tight coupling condition is violated $q(\tau_1) < 1$, corresponding to an efficiency $\eta(\tau_1, \epsilon_1) < \eta_{CA}$. To summarize, extending the space of parameters, e.g. by allowing τ to vary, may permit to find a larger maximum power, but this does not guarantee that the corresponding efficiency would be closer to the CA efficiency.

V. CONCLUSIONS

We have studied the thermodynamic properties of a model engine. The essential distinguishing features of our system are: 1) a realistic gas-like dynamics occurring in a spatially extended domain (i.e. the space between the moving piston and the thermostat); 2) inertial effects which allow for a larger freedom in the choice of parameters (e.g. τ is not constrained by the piston's velocity) and a more rich phase diagram; 3) a cyclical protocol repeating in a finite time τ which is not related to the relative excursions of the pressure and temperature, δ and ϵ. The results of the simulations of the molecular model are compared to analytical and numerical solutions of a simplified, coarse-grained, equation, which yields a qualitatively similar picture. A clear scenario emerges from our study, where the relation between the fluxes (heat and work) and the thermodynamic forces do not depend trivially upon τ, as it appears, for instance, in the approximated expressions of the Onsager matrix, Eq. (26). Our model is appropriate to study the issues of finite-time thermodynamics in a case where the adiabatic limit ($\tau \to \infty$) and the linear regime (small thermodynamic forces) are disentangled. It would be interesting to check whether higher order terms in the expansion (in δ, ϵ) of the 2V model is able to reproduce the presence (observed both in the non-linear 2V model and the MM) of a global maximum of the power. An interesting future extension of the present study is taking into account more realistic molecular interactions. A promising line of investigation, in view of the finite number N of particles in the engine, concerns the study of fluctuations of heat and work and the consequent definition of a fluctuating efficiency [31], already partially discussed in [4].

Appendix A

For the sake of consistency, in this Appendix we prove Eq. (12) for the simple case of discrete phase space and time. This formula, which holds also if time and space are both continuous, has appeared many times in the literature (see e.g. Ref. [37] for a nice pedagogical derivation).

Let us consider a discrete Markov process with time-dependent transition probabilities $p(i \to j, t)$ satisfying the detailed balance (DB) condition

$$e^{-\frac{\mathcal{H}(i,\lambda_t)}{T_t}} p(i \to j, t) = e^{-\frac{\mathcal{H}(j,\lambda_t)}{T_t}} p(j \to i, t), \tag{A1}$$

for every value of i, j and t, where λ_t is an external time-dependent protocol and T_t the time-dependent temperature. The entropy production of the medium for a given trajectory $\{i_t\}_{t=0}^{\tau}$ reads [38]

$$\Sigma_m(\tau) = \log \frac{P[\{i_s\}_{s=0}^{\tau} | i_0]}{\tilde{P}[\{i_{\tau-s}\}_{s=0}^{\tau} | i_\tau]} \tag{A2}$$

where $\tilde{P}$ denotes the probability of the trajectory in a process with the time reversed protocol $\tilde{\lambda}_t = \lambda_{\tau-t-1}$. By expliciting Eq. (A2) and using DB one gets

$$\Sigma_m(\tau) = \log \frac{p(i_o \to i_1, \lambda_0) \dots p(i_{\tau-1} \to i_\tau, \lambda_{\tau-1})}{p(i_\tau \to i_{\tau-1}, \lambda_{\tau-1}) \dots p(i_1 \to i_0, \lambda_0)} = \\ = -\sum_{t=1}^{\tau} \frac{\mathcal{H}(i_t, \lambda_{t-1}) - \mathcal{H}(i_{t-1}, \lambda_{t-1})}{T_{t-1}}. \tag{A3}$$

At every step the energy difference of the system can be decomposed according to

$$\Delta E = \mathcal{H}(i_t, \lambda_t) - \mathcal{H}(i_{t-1}, \lambda_{t-1}) = W_t + Q_t, \qquad \text{(A4)}$$

where the work W_t is the contribution due only to the change of λ, $W_t = \mathcal{H}(i_t, \lambda_t) - \mathcal{H}(i_t, \lambda_{t-1})$, and the heat Q_t is due to the change of state at fixed λ, $Q_t = \mathcal{H}(i_t, \lambda_{t-1}) - \mathcal{H}(i_{t-1}, \lambda_{t-1})$. Consequently

$$\Sigma_m(\tau) = -\sum_{t=0}^{\tau-1} \frac{Q_t}{T_t}. \qquad \text{(A5)}$$

The non-negative total entropy production $\Sigma_{tot}(\tau)$ [14] is the sum of the medium entropy production Σ_m and the system entropy production

$$\Sigma_s(\tau) = -\log \frac{\rho(i_0, t=0)}{\rho(i_\tau, t=\tau)}, \qquad \text{(A6)}$$

where $\rho(i_t, t)$ is the probability distribution function (pdf) of the system at time t. If λ_t and T_t are periodic function of time with period τ, there exists a periodic "stationary" pdf ρ_∞ such that $\rho_\infty(i, t) = \rho_\infty(i, t+\tau)$, for every i and t. This also means that if the initial pdf $\rho(i, t=0) = \rho_\infty(i, t=0)$, on average, the system entropy production vanishes, $\langle \Sigma_s \rangle = 0$ and finally

$$\langle \Sigma(\tau) \rangle = \langle \Sigma_m \rangle = -\sum_{t=0}^{\tau} \frac{\langle Q \rangle}{T_t}, \qquad \text{(A7)}$$

which is the discrete time equivalent of Eq. (12).

[1] S. Carnot, *Réflexions sur la puissance motrice du feu et sur les machines propres à développer cette puissance* (Bachelier Paris, 1824).
[2] C. Van den Broeck, Phys. Rev. Lett. **95**, 190602 (2005).
[3] T. Schmiedl and U. Seifert, EPL (Europhysics Letters) **81**, 20003 (2008).
[4] L. Cerino, A. Puglisi, and A. Vulpiani, Phys. Rev. E **91**, 032128 (2015).
[5] B. Andresen, R. Berry, A. Nitzan, and P. Salamon, Physical Review A **15**, 2086 (1977).
[6] F. Curzon and B. Ahlborn, American Journal of Physics **43**, 22 (1975).
[7] M. Esposito, K. Lindenberg, and C. Van den Broeck, Physical Review Letters **102**, 130602 (2009).
[8] M. Esposito, R. Kawai, K. Lindenberg, and C. Van den Broeck, Physical Review Letters **105**, 150603 (2010).
[9] R. Klages, W. Just, and C. Jarzynski, eds., *Nonequilibrium Statistical Physics of Small Systems: Fluctuation Relations and Beyond* (Wiley, 2013).
[10] P. Gaspard, Phys. A: Math. Gen. **369**, 201 (2006).
[11] U. M. B. Marconi, A. Puglisi, L. Rondoni, and A. Vulpiani, Physics Reports **461**, 111 (2008).
[12] U. Seifert, Rep. Prog. Phys. **75**, 126001 (2012).
[13] K. Sekimoto, *Stochastic energetics* (Springer Verlag, 2010).
[14] U. Seifert, Physical Review Letters **95**, 040602 (2005).
[15] A. Puglisi and D. Villamaina, Europhys. Lett. **88**, 30004 (2009).
[16] A. Celani, S. Bo, R. Eichhorn, and E. Aurell, Physical Review Letters **109**, 260603 (2012).
[17] M. Bauer, K. Brandner, and U. Seifert, "Optimal performance of periodically driven, stochastic heat engines under limited control," (2016), arxiv:1602.04119.
[18] R. Burioni, D. Cassi, F. Cecconi, and A. Vulpiani, Proteins **55**, 529 (2004).
[19] Y. Izumida and K. Okuda, Europhys. Lett. **83**, 60003 (2008).
[20] Y. Izumida and K. Okuda, Phys. Rev. E **80**, 021121 (2009).
[21] M. Falcioni, D. Villamaina, A. Vulpiani, A. Puglisi, and A. Sarracino, American Journal of Physics **79**, 777 (2011).
[22] L. Cerino, G. Gradenigo, A. Sarracino, D. Villamaina, and A. Vulpiani, Physical Review E **89**, 42105 (2014).
[23] E. H. Lieb, Physica A **263**, 491 (1999).
[24] C. Gruber and A. Lesne, in *Encyclopedia of Mathematical Physics* (Elsevier Amsterdam, 2006).
[25] M. Cencini, L. Palatella, S. Pigolotti, and A. Vulpiani, Phys. Rev. E **76**, 051103 (2007).
[26] M. Itami and S. Sasa, J. Stat. Phys. **158**, 37 (2015).
[27] C. Jarzynski, C. R. Physique **8**, 495 (2007).
[28] D. Chiuchiù and G. Gubbiotti, arXiv preprint, arXiv:1512.07464, (2015).
[29] T. G. Sano and H. Hayakawa, arXiv preprint, arxiv:1412.4468, (2014).
[30] M. Polettini, G. Verley, and M. Esposito, Phys. Rev. Lett. **114**, 050601 (2015).
[31] G. Verley, M. Esposito, T. Willaert, and C. Van den Broeck, Nature Communications **5**, 4721 (2014).
[32] S. de Groot and P. Mazur, *Non-equilibrium Thermodynamics* (Dover, 1984).
[33] K. Proesmans and C. Van den Broeck, Phys. Rev. Lett. **115**, 090601 (2015).
[34] K. Proesmans and C. Van den Broeck, J. Stat. Mech. , 023202 (2016).
[35] K. Brandner, K. Saito, and U. Seifert, Phys. Rev. X **5**, 031019 (2015).
[36] K. Proesmans, C. Driesen, B. Cleuren, and C. Van den Broeck, Phys. Rev. E **92**, 032105 (2015).
[37] Z. Gong and H. T. Quan, Phys. Rev. E **92**, 012131 (2015).
[38] J. Lebowitz and H. Spohn, J. Stat. Phys. **95**, 333 (1999).